



**IJPPR**

INTERNATIONAL JOURNAL OF PHARMACY & PHARMACEUTICAL RESEARCH  
An official Publication of Human Journals

ISSN 2349-7203




**Human Journals**

Research Article


February 2015 Vol.:2, Issue:3

© All rights are reserved by Maya Georgieva et al.

## ZINDO/S Computations of Absorption Bands in the UV Spectra of Some N4-Substituted Aralkylpiperazines with Antiproliferative Activity



**IJPPR**  
INTERNATIONAL JOURNAL OF PHARMACY & PHARMACEUTICAL RESEARCH  
An official Publication of Human Journals



**Lily Andonova<sup>1</sup>, Georgi Momekov<sup>2</sup>, Maya Georgieva<sup>1\*</sup>, Alexander Zlatkov<sup>1</sup>**

<sup>1</sup> *Department of Pharmaceutical Chemistry, Faculty of Pharmacy, Medical University of Sofia, Sofia, Bulgaria*

<sup>2</sup> *Department of Pharmacology, Pharmacotherapy and Toxicology, Faculty of Pharmacy, Medical University of Sofia, Sofia, Bulgaria*

**Submission:** 20 January 2015  
**Accepted:** 1 February 2015  
**Published:** 25 February 2015

**Keywords:** ZINDO/S calculations, aralkylpiperazines, antiproliferative activity

### ABSTRACT

The interpretation of the UV spectra of six N4-substituted aralkylpiperazines was based on ZINDO/S calculations performed on PM3 geometries. The calculated UV spectra correspond to the experimentally observed. Molecular orbital coefficients analysis suggest that electronic transitions are assigned to  $\pi \rightarrow \pi^*$  type. The negative values of HOMO and LUMO energies show that tested compounds have the properties of reductors, which is consistent with the previously proven antioxidant activity. A detailed cytotoxicity screening was performed in a panel of tumor cell lines after 72 h exposure using the MTT-dye reduction assay and the IC<sub>50</sub> values were calculated. The obtained results firmly indicate that the presented arylpiperazine derivatives exhibit antiproliferative effects in a panel of human tumor cell lines.



HUMAN JOURNALS

[www.ijppr.humanjournals.com](http://www.ijppr.humanjournals.com)

## INTRODUCTION

Piperazine nucleus is one of the most important heterocycles exhibiting remarkable pharmacological activities. Even slight change in substitution pattern in piperazine nucleus, including the introduction of arylalkyl substituent causes distinguishable difference in their pharmacological activities such as antipsychotic, anticonvulsant, antiarrhythmic, antimicrobial, antimalarial, cytotoxic, anxiolytic, antidepressant, procognitive and antioxidant effects [1-4].

The general chemical structure of these compounds contain aralkylpiperazine as a core fragment and an alkyl chain with two to four methylene units, attached to the N4 atom of the piperazine moiety, and ending with a terminal amide or an imide fragment. In the recent years, there has been a great interest in developing aralkylpiperazines containing a methylxanthine moiety as a terminal fragment. This is due to the various biological activities and well-known clinical use of methylxanthines as bronchodilators, psychostimulants, diuretics, vasodilators, antiviral and antitumor agents. Furthermore some methylxanthines modulate the cytotoxicity of conventional antitumor drugs [5-8].

Studying of the electronic structure of compounds by UV spectral and quantum chemical methods is important, not only for interpretation of the spectra, but also to estimate of direction of the electronic density's redistribution of the compounds, which is a determining factor of their reactivity and biological activity. Spectroscopic techniques when combined with quantum chemical calculations are emerging as one of the most powerful tools to study the dynamical behavior and to gain an insight into the electronic and molecular structures of natural products at microscopic level [9, 10].

In the current study, the electronic structure of some aryl/aralkyl substituted piperazine derivatives, containing methylxanthine moiety with antioxidant activity was studied, using UV spectra and quantum chemical calculations. Their antiproliferative effects were also evaluated.

## MATERIALS AND METHODS

The UV spectra were recorded in ethanol solution using 1 cm quartz cells on a Hewlet Packard 8452A Diode Array Spectrophotometer equipped with an HP Vectra 386/25 computer at concentration  $10^{-5} \text{ mol.L}^{-1}$ .

### Computational details

The MO calculations have been performed using the Hyper Chem 7.50 software [11]. For ZINDO/S (Zerner's Inter-mediate Neglect of Differential Overlap/Spectroscopy) calculations of the singlet electronic transitions, configuration interaction between six occupied and unoccupied MO's have been selected (CI matrix included 77 to 91 singly excited configurations). The ground state geometry was optimized by PM3/RHF method (RHF stands for Restricted Hartree–Fock) [15]. A root-mean-square (RMS) gradient in the energy of 0.005 kcal.Å.mol<sup>-1</sup> was used as a criterion for choosing an optimized conformation along with the Polak–Ribiere conjugate gradient algorithm [11, 16]. For calculation of one-electron two-center resonance integrals, the overlap weighting factors are used as follows:  $f_{\sigma} = 1.267$  and  $f_{\pi} = 0.585$ . The UV–Vis spectra were calculated with the SWizard program, revision 5.0 [17, 18]. The absorption profiles were calculated using pseudo–Voigt model, which is convolution of both the Gaussian and Lorentzian functions (with weights  $W$  and  $1-W$  respectively):

$$\varepsilon(\omega) = W \cdot c_1 \sum_I \frac{f_I}{\Delta_{1/2,I}} \exp \left( -2.773 \frac{(\omega - \omega_I)}{\Delta_{1/2,I}} \right) + (1 - W) c_2 \sum_I \frac{f_I}{\Delta_{1/2,I}} \cdot \frac{0.25 \Delta_{1/2,I}^2}{(\omega - \omega_I)^2 + 0.25 \Delta_{1/2,I}^2}$$

Where molar absorptivity ( $\varepsilon$ ) is given in dimension mol<sup>-1</sup>.L.cm<sup>-1</sup>, energies ( $\omega_I$ ) and half-bandwidths ( $\Delta_{1/2,I}$ ) are expressed in cm<sup>-1</sup>. The sums in the equation also include all allowed electronic transitions and oscillator strengths ( $f_I$ ). The average half-bandwidth ( $\Delta_{1/2,I}$ ) for all bands were taken to be equal to 3000 cm<sup>-1</sup> as a good approximation for all of studied electronic transitions [17]. All computations were carried out on a PC with Intel Pentium dual–core CPU E6500 at 2.93 GHz and 4 GB RAM under Windows 7 operating systems.

### Drugs, chemicals and reagents

Formic acid, 2-propanol, and L-glutamine were purchased from AppliChem GmbH, (Darmstadt, Germany). Fetal calf serum (FCS) and RPMI-1640 medium were purchased from Sigma–Aldrich GmbH (Steinheim, Germany). The cell culture flasks and the flat-bottomed multi-well plates were obtained from Nunc A/S (Kamstrupvej, Denmark). The tetrazolium salt 3-(4,5-dimethylthiazol-2-yl)-2,5-diphenyl tetrazolium bromide (MTT) was supplied from Merck

(Darmstadt, Germany). The referent antineoplastic drug cisplatin was used as a commercially available pharmaceutical grade substance.

### **Cell lines and culture conditions**

The human tumor cell lines, used in this study namely SKW-3, human T-cell chronic lymphocytic leukemia, originally described to be established from the peripheral blood of a 61-years old man with T-cell chronic lymphocytic leukemia (CLL) in 1977; however, DNA fingerprinting and cytogenetic analysis showed cross contamination with cell line KE-37; KE-37 was established from a 27 years old man with acute lymphoblastic leukemia (ALL) in 1979; HL 60 human acute myeloid leukemia (AML), established from the peripheral blood of a 35 years old woman with acute myeloid leukemia (AML FAB M2) in 1976; cells are apparently tetraploid derivatives of the hypodiploid original; REH-human B-cell precursor leukemia established from the peripheral blood of a 15 years old North African girl with acute lymphoblastic leukemia (ALL at first relapse) in 1973; carries t (12;21) leading to ETV6-RUNX1 (TEL-AML1) fusion gene. The cell lines were obtained from the German Collection of Microorganisms and Cell Cultures (DSMZ GmbH, Braunschweig, Germany). They were maintained as suspension type cultures in a controlled environment-RPMI-1640 medium, supplemented with 10% heat-inactivated fetal calf serum and 2 mM L-glutamine, at 37 °C in a 'Heraeus' incubator with 5% CO<sub>2</sub> humidified atmosphere. In order to maintain the cells in log phase cellular suspension aliquots were refed with fresh RPMI-1640 medium two or three times per week.

The stock solution of the referent antineoplastic agent cisplatin was prepared using the commercially available sterile dosage forms for clinical application, while the tested arylpiperazines were dissolved in DMSO. The stock solutions were consequently diluted with RPMI-1640 medium to yield the desired final concentrations (in case of DMSO stocks at the final dilutions obtained, the concentration of the solvent never exceeded (0.5%).

All of the procedures concerning the cell culture maintenance, drug dissolution and treatment were carried out in a 'Heraeus' Laminar flow cabinet.

### **Cytotoxicity assessment (MTT-dye reduction assay)**

The cellular viability was assessed using the MTT-dye reduction assay as described by Mosmann with slight modifications [19, 20]. The assay is based on the reduction of the yellow tetrazolium dye MTT to a violet formazan product *via* the mitochondrial succinate dehydrogenase in viable cells. In brief, exponentially growing cells were seeded in 96 well flat bottomed microplates (100  $\mu$ l/well) at a density of  $1 \times 10^5$  cells per ml and after 24 h incubation at 37°C they were exposed to graded concentrations of the tested compounds for 72 h. For each concentration a set of at least 8 wells were used. After the exposure period 10  $\mu$ l MTT solution (10 mg/ml in PBS) aliquots were added to each well. Thereafter the microplates were incubated for 4 h at 37°C and the MTT-formazan crystals formed were dissolved through addition of 100  $\mu$ l/well 5 % formic acid solution in 2-propanol. The MTT-formazan absorption was determined using a microprocessor controlled microplate reader (Labexim LMR-1) at 580 nm.

#### Bioassay data processing and statistics

The cell survival data were normalized as percentage of the untreated control (set as 100 % viability), were fitted to sigmoidal dose response curves and the corresponding IC<sub>50</sub> values (concentrations causing 50 % suppression of cellular viability) were calculated using non-linear regression analysis (Graphpad Prizm Software for PC). The statistical processing of biological data included the Student's t-test whereby values of  $p \leq 0.05$  were considered as statistically significant.

## RESULTS AND DISCUSSION

The synthesis and structural evaluation of compounds 1–6 (Fig. 1) was discussed in our previous publication [21]. In addition, this paper presents the experimental and theoretical studies of the electronic absorption spectra of the previously obtained piperazine derivatives with antioxidant activity.

Some quantum chemical parameters such as total energy (TE); binding energy (BE); heat of formation (HF), dipole moments ( $\mu$ ), energy of highest occupied molecular orbital (HOMO), energy of lowest unoccupied molecular orbital (LUMO) as well as HOMO/LUMO gap of theobromine (Tb) and compounds 1–6 were calculated using PM3 method, in order to evaluate their chemical properties and possibilities to interact with biological macromolecules (receptors, enzymes) and the corresponding results are presented in Table 1.

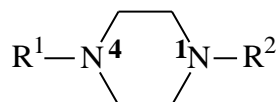
**Table 1. Quantum chemical parameters of Tb and compounds 1–6 were calculated using PM3/RHF method**

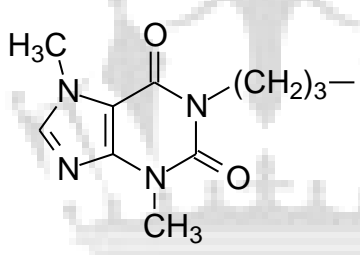
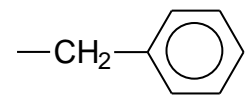
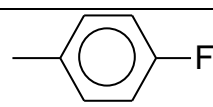
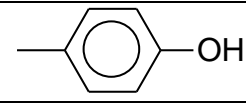
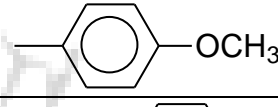
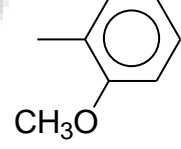
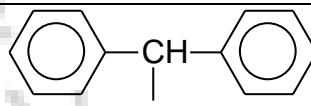
	<b>Tb</b>	<b>1</b>	<b>2</b>	<b>3</b>	<b>4</b>	<b>5</b>	<b>6</b>
<b>TE [eV]</b>	–2189.299	–4480.96 2	–4905.86 4	–4774.852	–4923.744	–4923.740	–5252.741
<b>BE [eV]</b>	–96.926	–254.636	–254.999	–259.178	–270.692	–270.688	–306.728
<b>HF [eV]</b>	–2.209	–1.187	–3.77	–3.147	–2.732	–2.727	0.221
<b>μ [D]</b>							
<b>x</b>	–3.240	3.760	4.059	4.836	–3.717	3.313	3.678
<b>y</b>	2.934	–0.538	0.624	–0.143	–1.957	–1.223	–1.042
<b>z</b>	0.000	–0.306	–1.471	–0.305	0.282	0.031	–0.510
<b>Total</b>	4.371	3.811	4.362	4.848	4.210	3.531	3.856
<b>E<sub>H</sub> [eV]</b>	–8.845	–8.302	–8.392	–8.024	–8.326	–8.137	–8.147
<b>E<sub>L</sub> [eV]</b>	–0.584	–0.491	–0.514	–0.504	–0.503	–0.469	–0.494
<b>ΔE<sub>H/L</sub> [eV]</b>	7.901	7.811	7.878	7.520	7.823	7.668	7.653

TE –Total Energy; BE – Binding Energy; HF – Heat of Formation; μ– Dipole moments, E<sub>H</sub>–E<sub>HOMO</sub>, E<sub>L</sub>–E<sub>LUMO</sub>, ΔE<sub>H/L</sub>– HOMO/LUMO gap

It is well known, that the HOMO/LUMO energy gap is an important stability index. Also the high value of HOMO/LUMO gap of the tested compounds reflect the chemical stability of the molecules. The results show that the calculated energy values of the studied compounds are comparable and their stability is nearly the same. Compound 6 slightly deviates from this trend but without exception. The observed HOMO/LUMO energy gap of 7.52–7.90 eV (Table 1) is a scale to assess their redox potential which is substantial for the metabolism of those compounds, such as oxidative reactions in the presence of Cytochrome P450 enzymes. The frontier molecular orbitals are important in determination of the ability of a molecule to absorb light and molecular reactivity. The vicinal orbitals of HOMO and LUMO play role of an electron donor and an electron acceptor respectively. Thus the lower negative HOMO energy and the negative values of LUMO energies show that these compounds have the properties of reductors. These data are

consistent with the proven antioxidant activity of compounds 1-6 [21]. This information may be significant for drug metabolism, as the oxidation and the reduction are the main metabolic pathways for many drug molecules.



Compound	R <sup>1</sup>	R <sup>2</sup>
1		
2		
3		
4		
5		
6		

**Fig. 1. Structures of studied N4-substituted aralkylpiperazines 1-6**

The biochemical reactivity of a drug is in a direct consequence of its electronic structure. The most straight forward manifestation of the electronic structure of a molecule is its electronic absorption spectrum. Thus, in order to clarify the influence of the electronic properties on the expressed biological activity of the target compounds, their experimental and theoretically calculated electronic spectra were defined. The results from the experimental electronic spectra measured in ethanol solution along with the calculated electronic transitions with high oscillatory strength are listed in Table 2.

**Table 2. Comparison between the experimental and theoretical UV spectral data of Tb and compounds 1-6**

Compound	$\lambda_{\max}$ exp [nm]	$\lambda_{\max}$ calc[nm]	Individual excitation states [nm]	Energy of electronic transition [eV]	Oscillator strength	Orbitals involved in electronic transitions <sup>a</sup>
Tb	272	288	288.4	4.30	0.4380	H-0 $\rightarrow$ L+0 (+97%)
	230	238	252.4	4.91	0.0639	H-0 $\rightarrow$ L+2 (+60%) H-0 $\rightarrow$ L+1 (+26%)
	205	212	237.7	5.22	0.0129	H-5 $\rightarrow$ L+0 (+40%) H-5 $\rightarrow$ L+2 (+33%)
			237.6	5.22	0.1564	H-0 $\rightarrow$ L+1 (+72%) H-0 $\rightarrow$ L+2 (+24%)
			223.1	5.56	0.0002	H-0 $\rightarrow$ L+3 (+96%)
			212.4	5.84	0.3757	H-2 $\rightarrow$ L+0 (+80%)
			205.6	6.03	0.0030	H-5 $\rightarrow$ L+0 (+29%) H-5 $\rightarrow$ L+2 (+25%)
			194.1	6.39	0.0062	H-0 $\rightarrow$ L+5 (+94%)
			193.8	6.40	0.0729	H-0 $\rightarrow$ L+4 (+75%)
1	274	281	281.2	4.41	0.5830	H-1 $\rightarrow$ L+0 (100%)
	210	243	271.8	4.56	0.0013	H-5 $\rightarrow$ L+0 (+81%)
		213	268.6	4.62	0.0044	H-0 $\rightarrow$ L+3 (35%) H- 2 $\rightarrow$ L+4 (+21%)
			243.6	5.09	0.2551	H-1 $\rightarrow$ L+2 (+84%)
			237.9	5.21	0.0352	H-1 $\rightarrow$ L+1 (83%)
			217.8	5.69	0.0044	H-1 $\rightarrow$ L+5 (+100%)
			213.3	5.81	0.0793	H-0 $\rightarrow$ L+4 (61%)
			206.6	6.00	0.0008	H-0 $\rightarrow$ L+0 (+67%)
			194.5	6.37	0.0017	H-5 $\rightarrow$ L+1 (+96%)
			193.0	6.42	0.1749	H-3 $\rightarrow$ L+4 (24%)
2	272	281	281.3	4.41	0.5861	H-1 $\rightarrow$ L+0 (+99%)
	238	243	275.0	4.51	0.0103	H-0 $\rightarrow$ L+4 (+45%) H-3 $\rightarrow$ L+3 (+30%)
	208	220	271.4	4.57	0.0013	H-5 $\rightarrow$ L+0 (+81%)
			243.6	5.09	0.2539	H-1 $\rightarrow$ L+2 (83%)
			237.9	5.21	0.0349	H-1 $\rightarrow$ L+1 (+83%)
			220.1	5.63	0.1563	H-0 $\rightarrow$ L+3 (+76%)
			217.8	5.69	0.0044	H-1 $\rightarrow$ L+5 (+100%)
			204.0	6.08	0.0010	H-0 $\rightarrow$ L+0 (+62%) H-2 $\rightarrow$ L+0 (27%)



			196.4	6.31	0.0500	H-2→L+3 (+48%)
			195.5	6.34	0.2067	H-0 →L+4 (42%)
			194.6	6.37	0.0015	H-2→L+4 (+28%)
						H-5→L+1 (96%)
3	276	281	281.4	4.41	0.5479	H-1 → L+0 (86%)
	228	243	280.3	4.42	0.0642	H-0 →L+3 (+55%)
	198	225	271.6	4.56	0.0013	H-3→L+4 (26%)
			243.6	5.09	0.2547	H-5→L+0 (+81%)
			237.9	5.21	0.0355	H-1→L+2 (+84%)
			224.7	5.52	0.2210	H-1→L+1 (+83%)
			217.8	5.69	0.0045	H-0→L+4(+87%)
			209.4	5.92	0.0004	H-1→L+5 (+100%)
			196.3	6.32	0.0008	H-0 →L+0 (+75%)
			194.5	6.37	0.0020	H-2→L+0 (59%) H-0 →L+0 (+24%)
			193.5	6.41	0.2525	H-5→L+1 (96%)
						H-2→L+4 (+31%)
			192.3	6.45	0.1569	H-2→L+3 (+23%)
						H-0→L+3 (+22%)
4	272	283	283.5	4.37	0.4721	H-2→L+4 (+36%)
	240	243	278.2	4.46	0.0689	H-2→L+3 (+26%)
	208	222	271.2	4.57	0.0065	H-1 → L+0 (+93%)
			244.1	5.08	0.2187	H-0→L+3 (59%) H-2→L+4 (+32%)
			239.6	5.17	0.0345	H-5→L+0 (+81%)
			230.0	5.39	0.0004	H-1→L+2 (86%)
			221.9	5.59	0.2159	H-1→L+1 (89%)
			217.4	5.70	0.0085	H-0 → L+0 (+93%)
			201.7	6.15	0.0055	H-0 →L+4 (81%)
			200.0	6.20	0.0057	H-1→L+5 (95%)
			192.7	6.43	0.0072	H-2→L+0 (53%) H-3→L+0 (43%)
						H-3→L+0 (+52%)
5	274	281	281.1	4.41	0.5821	H-2→L+0 (44%)
	240	243	277.3	4.47	0.0078	H-5→L+1 (+94%)
	210	222	272.0	4.56	0.0013	H-1 → L+0 (100%)
			243.6	5.09	0.2530	H-0→L+3 (45%)
			237.9	5.21	0.0361	H-5→L+0 (+81%)
			222.4	5.57	0.0676	H-1→L+2 (+84%)
			217.7	5.70	0.0047	H-1→L+1 (+84%)
						H-0 →L+4 (61%)
						H-1→L+5 (100%)

			208.8	5.94	0.0006	H-0 → L+0 (+55%) H-2→L+0 (+24%)
			201.0	6.17	0.4342	H-2→L+4 (+38%) H-0→L+3 (+36%)
			196.2	6.32	0.4115	H-2→L+3 (+41%) H-0 →L+4 (29%)
			195.2	6.35	0.0006	H-0 → L+0 (+44%) H-2→L+0 (37%)
			194.4	6.38	0.0015	H-5→L+1 (+96%)
6	272	281	281.0	4.41	0.5865	H-1 → L+0 (100%)
	208	244	247.1	5.02	0.0708	H-1→L+2(82%)
		216	244.3	5.08	0.1040	H-0 →L+5 (+46%)
			243.7	5.09	0.2667	H-1→L+2 (+85%)
			237.7	5.22	0.0363	H-1→L+1 (+85%)
			216.6	5.72	0.1889	H-0→L+3 (+77%)
			203.6	6.09	0.0001	H-0 → L+0 (+59%) H-2→L+0 (33%)
			201.9	6.14	0.0306	H-2→L+3 (34%)
			194.3	6.38	0.4048	H-3→L+3 (+28%) H-0 →L+4 (+25%)
			194.2	6.38	0.0003	H-2→L+0 (+45%) H-0 → L+0 (+39%)
			192.0	6.46	0.8763	H-2→L+3 (+29%)

<sup>a</sup>Only the major singlet excitations are reported. Their percentage contributions to wave functions of excited states are given in parenthesis.

In addition the contribution of the individual absorption bands to the corresponding excitation state for each of the evaluated compounds was determined. The theoretical spectra of theobromine (Tb) and compounds 1-6 (upper line in black) together with the defined contribution of the individual absorption bands of calculated electronic excitation states (in color) are presented on Fig. 2.

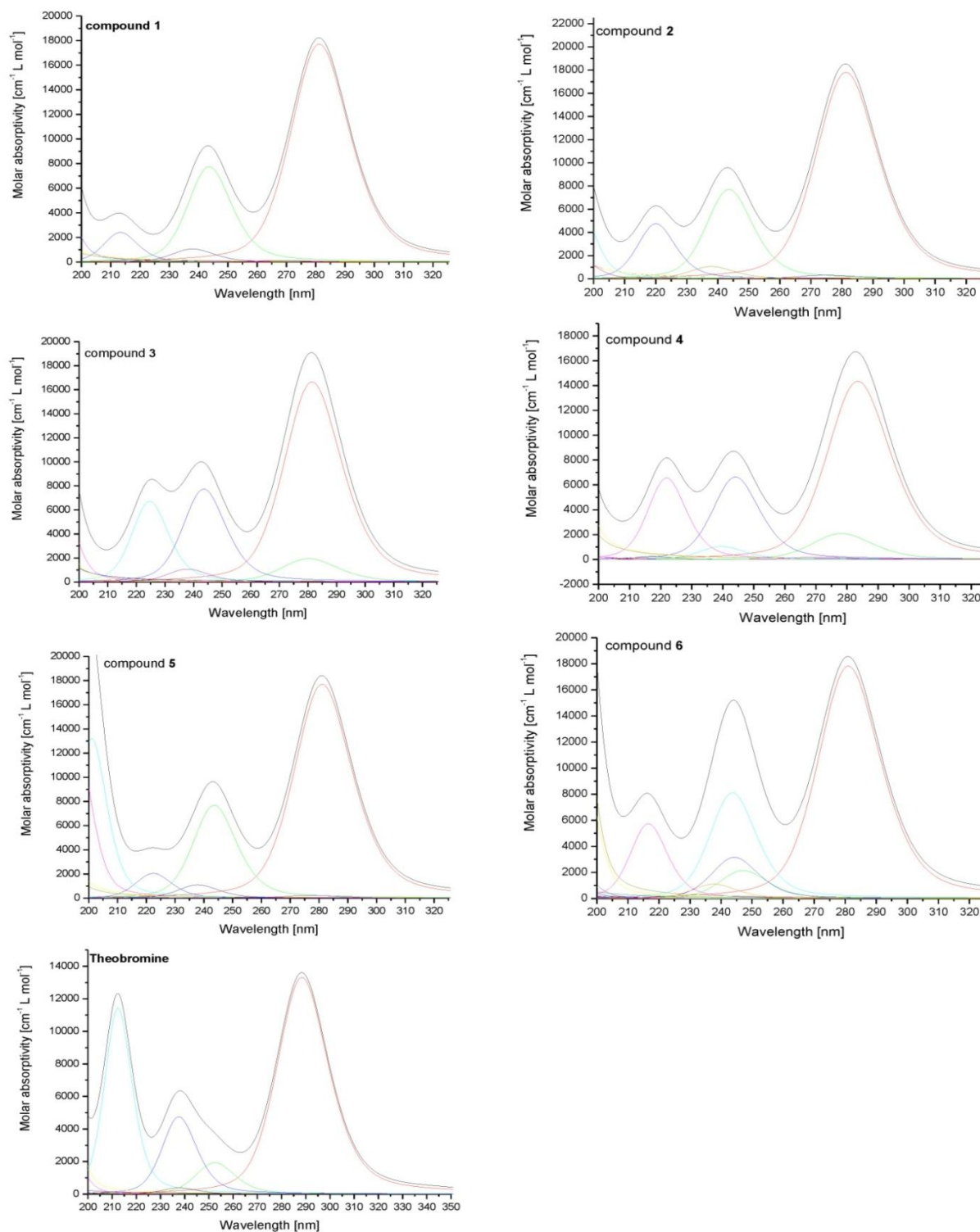


**Fig. 2. Theoretical UV spectra of theobromine (Tb) and compounds 1-6 (in black) together with contribution of individual absorption bands of calculated electronic excitation states (in color)**

On the obtained electronic spectra of the tested compounds, recorded at concentration  $1.10^{-5}$  mol.L<sup>-1</sup> is visible that they exhibit in general three characteristic absorption bands at 272 – 276 nm, at 198 – 208 nm and at 228 – 240 nm. We observed, that the last band lacks in the spectra of 1 and 6. At the same conditions, Tb shows absorption peaks at 272 nm and slight rise in absorbance at about 230 nm. The general absorption band corresponds to "x"-band of the simple purines, while the absorption at about 230 nm can be attributed to "y"-band of the simple purines [22].

The interpretation of the spectra was based on ZINDO/S calculations performed on PM3 geometries and SWizard calculations and show that the investigated compounds have three theoretical absorption bands at 281–288 nm, at 243–244 nm and at 213–225 nm (Fig. 2). As can be seen from the theoretical spectrum of Tb the peak at 288 nm with corresponding excitation energy of 4.30 eV and oscillator strength 0.4380 is due to the electronic transition from HOMO to LUMO orbitals (H-0 → L+0). In the spectra of other compounds the HOMO orbital belongs to the aromatic system and this transition is mainly due to the H-1 → L+0 transition, which is identical with H-0 → L+0 transition in Tb and values of excitation energy and oscillator strength are almost identical to those of Tb (Table 2). The absorption at 238 nm in the theoretical spectrum of Tb is mainly due to transitions H-0 → L+1, H-0 → L+2. Transitions H-5 → L+0 and H-5 → L+2 also have some contribution to this absorption band. In the spectra of compounds 1-6, this absorption band is due to H-1 → L+2 (5.09 eV) and H-1 → L+1 (5.21 eV) transitions, which belong to orbitals from the xanthine ring. The third absorption peak in the theoretical spectrum of Tb at 212 nm is due to H-2 → L+0 transition (5.84 eV). In the spectra of the rest of the investigated compounds, this peak is observed at 216-225 nm and corresponds to the H-0 → L+4 transition (for 2 and 6 H-0 → L+3 transition) and has excitation energy 5.52 – 5.81 eV.

The performed molecular orbital coefficients analysis and obtained molecular orbital plots for the targeted structures indicate that molecular orbitals involved in transitions are mainly composed of p-atomic orbitals, therefore the absorptions correspond to  $\pi \rightarrow \pi^*$  type of electronic transitions. It can be said that the type of the electronic absorption spectra of the tested compounds are due to electronic transitions mainly in xanthine fragment of the structures. The

differences between theoretical and experimental UV spectra are probably due to vibration effects and H-bonding with the solvent molecules.

### Cytotoxic/antiproliferative effects of the investigated newly synthesized arylpiperazines

The antiproliferative/cytotoxic effects of the tested series of arylpiperazines were evaluated using the standard MTT-dye reduction assay after 72 hours of exposure on human tumor cell lines SKW-3 (T-cell chronic lymphocytic leukemia), HL-60 (acute myeloid leukemia), REH (B-cell precursor leukemia). Clinically applied cytostatic drug cisplatin was used as a positive control. The obtained experimental data were fitted to concentration–effect sigmoid curves and the corresponding  $IC_{50}$  (the concentration leading to 50% reduction of the cellular viability) values were calculated, using a non-linear regression analysis. The calculated inhibitory concentrations are summarized in Table 3.

**Table 3.MTT-bioassay data for the tested arylpiperazines against a panel of human tumor cell lines.**

Compound	$IC_{50}$ ( $\mu$ M)		
	HL-60	SKW-3	REH
1	> 400,0	391,1 $\pm$ 24,9	264,1 $\pm$ 19,9
2	308,8 $\pm$ 21,1	155,5 $\pm$ 10,1	260,3 $\pm$ 22,8
3	381,7 $\pm$ 17,9	329,3 $\pm$ 14,4	393,1 $\pm$ 30,1
4	331,1 $\pm$ 14,2	209,7 $\pm$ 19,7	247,4 $\pm$ 22,4
5	> 400,0	382,5 $\pm$ 17,8	298,9 $\pm$ 26,7
6	33,7 $\pm$ 5,4	33,2 $\pm$ 2,6	40,67 $\pm$ 5,2
Cisplatin	8,1 $\pm$ 0,9	11,9 $\pm$ 2,3	23,6 $\pm$ 4,1

The tested compounds demonstrated concentration dependent antiproliferative activity (Fig 3.). The highest cytotoxic effect was observed for compound 6 and it is comparable with the referent drug cisplatin. The rest of the compounds showed significantly lower activity. The cytotoxicity was encountered at concentrations exceeding 100  $\mu$ M.

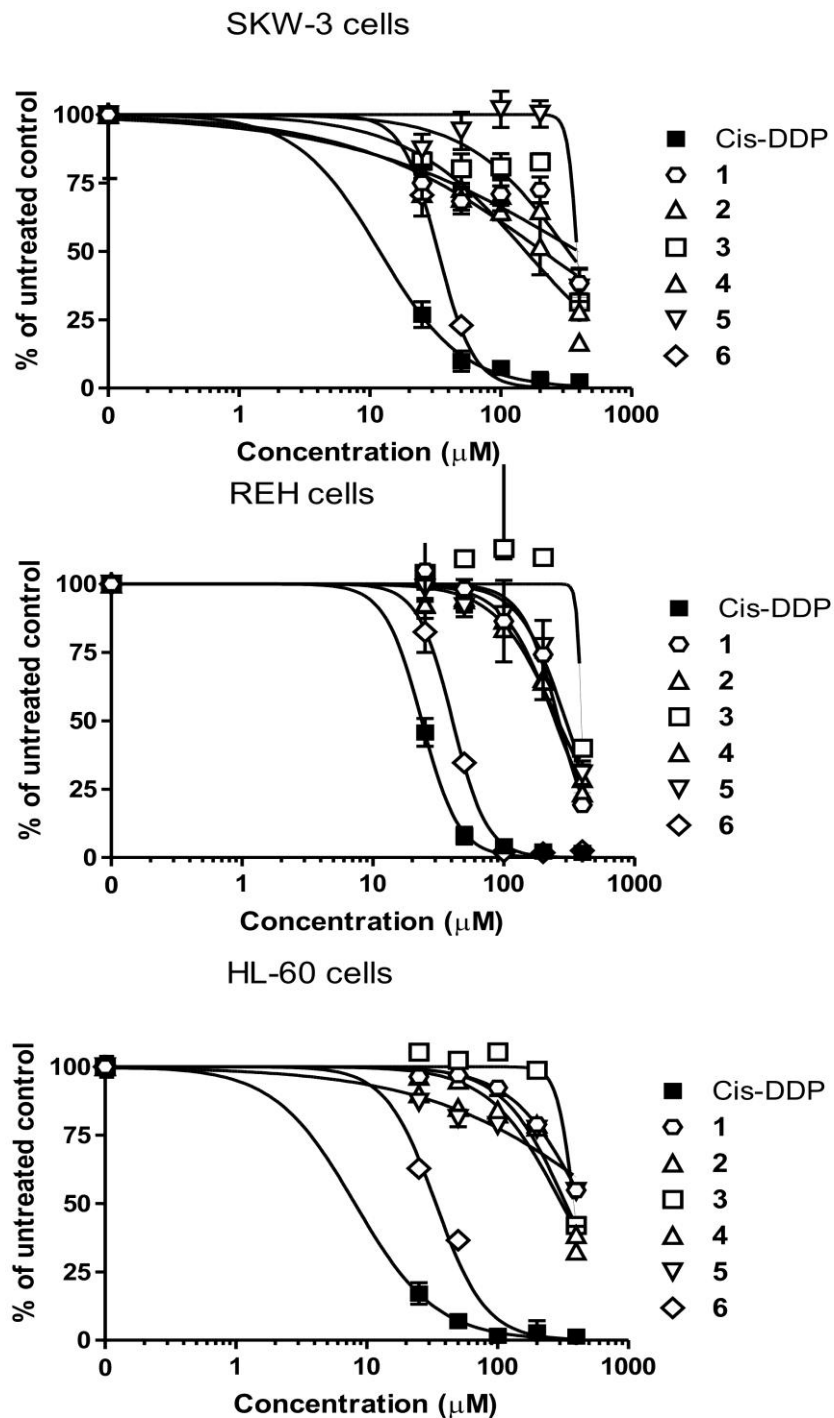


**Fig. 3.** Antiproliferative activity of the referent cytostatic drug cis-DDP and the investigated compounds 1-6 on the human tumor cell lines after 72 h of incubation (n=8; MTT-assay).

## CONCLUSION

The determined negative values of HOMO and LUMO energies show that the tested compounds have the properties of reductors, which is consistent with the previously proven antioxidant activity. Based on the obtained theoretical data, it may be concluded that the type of the electronic absorption spectra of the tested compounds is due to electronic transitions mainly in the xanthine fragment of the structure, whereas the corresponding molecular orbital coefficients analysis suggest that these electronic transitions are assigned to  $\pi \rightarrow \pi^*$  type. The observed differences between the theoretical and the experimental UV spectra are probably due to vibration effects and H-bonding of the evaluated structures with the solvent molecules.

A detailed cytotoxicity screening was performed in a panel of tumor cell lines after 72 h exposure using the MTT-dye reduction assay and the  $IC_{50}$  values were calculated. The obtained results firmly indicate that the presented arylpiperazine derivatives exhibit antiproliferative effects in a panel of human tumor cell lines. Compound 6 demonstrated the highest cytotoxic activity, comparable with the referent drug cisplatin. The proven cytotoxic activity of the series supported the well-established antineoplastic potential of arylpiperazine derivatives with xanthine moiety at  $N_4$ . This study has shown that the presented compounds exert antiproliferative potential and the combination of arylpiperazine and xanthine moiety is suitable and should be taken into consideration in further design of structures with potential antineoplastic properties.

## REFERENCES

1. Amita T, Mridula M, Manju V. Piperazine: the molecule of diverse pharmacological importance. *Inter J of Ayurand Pharm.* 2011; 2: 1547-1548.
2. Pietrzycka A, Stepniewski M, Waszkielewicz AM, Marona H. Preliminary evaluation of antioxidant activity of some 1-(phenoxyethyl)-piperazine derivatives. *Acta Pol Pharm.* 2006; 63(1): 19-24.
3. Salat K, Moniczewski A, Salat R, Janaszek M, Filipek B, Malawska B, Wieckowski K. Preliminary evaluation of antioxidant activity of some 1-(phenoxyethyl)-piperazine derivatives. *Pharmacol, Biochem and Beh.* 2012; 101: 138-147.
4. Becker OM, Dhanoa DS, Marantz Y, Chen D, Shacham S, Cheruku S, Heifetz A, Mohanty P, Fichman M, Sharadendu A, Nudelman R, Kauffman M, Noiman S. An integrated in silico 3D model-driven discovery of a novel, potent, and selective amidosulfonamide 5-HT<sub>1A</sub> agonist (PRX-00023) for the treatment of anxiety and depression. *J. Med. Chem.* 2006; 49: 3116-3135.
5. Boike GM, Petru E, Sevin BU, Averette HE, Chou TC, Penalver M, Donato D, Schiano M, Hilsenbeck SG, Perras J. Chemical enhancement of cisplatin cytotoxicity in a human ovarian and cervical cancer cell line. *Gynecologic Oncology.* 1990; 38(3): 315-322.
6. Husain A, Rosales N, Schwartz GK, Spriggs DR. Lisofylline Sensitizes p53 Mutant Human Ovarian Carcinoma Cells to the Cytotoxic Effects of cis-diamminedichloroplatinum (II). *Gynecologic Oncology.* 1998; 70(1): 17-22.



7. Smith KS, Folz BA, Adams EG, Bhuyan BK. Synergistic and additive combinations of several antitumor drugs and other agents with the potent alkylating agent adozelesin. *Cancer Chemotherapy and Pharmacology*. 1995;35(6):471-82.
8. Zlatkov AB, Peikov PT, Momekov GC, Pencheva I, Tsvetkova B. Synthesis, Stability and Computational Study of some Ester Derivatives of Theophylline-7-acetic Acid with Antiproliferative Activity. *Der Pharma Chemica*. 2010;2(6):197-210.
9. Srivastava A, Tandon P, Jain S, Asthana BP. Antagonistic properties of a natural product – Bicuculline with the gamma-aminobutyric acid receptor: Studied through electrostatic potential mapping, electronic and vibrational spectra using *ab initio* and density functional theory. *Spectrochim. Acta A*. 2011; 84 (1):144–155.
10. Joshi BD, Srivastava A, Tandon P, Jain S. Molecular structure, vibrational spectra and HOMO, LUMO analysis of yohimbine hydrochloride by density functional theory and *ab initio* Hartree–Fock calculations. *Spectrochim. Acta A*. 2011; 82 (1): 270–278.
11. HyperChem for Windows, Release 7.5 Professional Version, Hypercube Inc., Gainesville, Florida, USA, 2002.
12. Ridley J, Zerner MC. Intermediate neglect of differential overlap technique for spectroscopy—pyrrole and azines. *Theor. Chim. Acta*. 1973; 32(2): 111–134.
13. Ridley JE, Zerner MC. Triplet states via intermediate neglect of differential overlap: benzene, pyridine and the diazines. *Theor. Chim. Acta (Berl.)* 1976; 42:223–236.
14. Ridley J, Zerner MC. The calculated spectra of the azanaphthalenes. *J. Mol. Spectrosc.* 1974;50(1–3): 457–473.
15. Stewart JJP. Optimization of parameters for semiempirical methods II. Applications. *J. Comp. Chem.* 1989;10(2): 221–264.
16. Stewart JJP. Optimization of parameters for semiempirical methods: I. Method. *J. Comput. Chem.* 1989; 10: 209–220.
17. Gorelsky SI. *SWizard program*, <http://www.sg-chem.net/>, University of Ottawa, Ottawa, Canada, 2013.
18. Gorelsky SI, Lever ABP. Electronic structure and spectra of ruthenium diimine complexes by density functional theory and INDO/S. Comparison of the two methods. *J. Organomet. Chem.* 2001; 635(1–2): 187–196.
19. Mosmann T. Rapid colorimetric assay for cellular growth and survival: application to proliferation and cytotoxicity assays. *J Immunol Methods*. 1983;65:55-63.
20. Konstantinov SM, Eibl H, Berger MR. BCR-ABL influences the antileukaemic efficacy of alkylphosphocholines. *Br J Haematol*. 1999;107:365-380.
21. Andonova L, Zheleva-Dimitrova D, Georgieva M, Zlatkov A. Synthesis and antioxidant activity of some 1-aryl/alkyl piperazine derivatives with xanthine moiety at N4. *Biotechnology & Biotechnological Equipment*. 2014;28(6): 1165–1171.
22. Mason SF. Purine studies. Part II. The ultra-violet absorption spectra of some mono- and poly-substituted purines. *J. Chem. Soc.* 1954; 2071-2081.